Local Kinetic Modeling of Aluminum Oxide Metal-Organic CVD From Aluminum Tri-isopropoxide

Hugues Vergnes, Diane Samélor, Alain Gleizes, Constantin Vahlas, Brigitte Caussat

Communication

DOI: 10.1002/cvde.201004301

Local Kinetic Modeling of Aluminum Oxide Metal-Organic CVD From Aluminum Tri-isopropoxide**

By *Hugues Vergnes*, *Diane Samélor*, *Alain N. Gleizes*, *Constantin Vahlas*,* and *Brigitte Caussat**

Due to numerous allotropic modifications and to the subsequent large spectrum of structure-properties relationships, aluminum oxides in the form of films and coatings are of major technological interest for a wide range of applications, e.g., optics and microelectronic components, wear resistance, catalyst support, protection against corrosion, and high temperature oxidation. Metal-organic (MO)CVD is a potentially attractive technique for the processing of such coatings, especially on complex-in-shape, temperature-sensitive parts. In this context, processing-structure relationships were established and the feasibility of such a process was proven, on the laboratory scale, in a series of papers recently published by the authors.[1–3] It is recalled that, using aluminum tri-isopropoxide (ATI) as the precursor and operating in a hot-wall reactor in the temperature range 350–415 °C, under 5 Torr, with dry N_2 as a carrier/dilution gas results in partially hydroxylated films $AlO_{1+x}(OH)_{1-2x}$; x varies from 0 (AlOOH) at 350 °C to 0.5 (Al_2O_3) at 415 °C. Films processed between 415 °C and 650 °C are composed of amorphous Al_2O_3; nanostructured gamma-alumina films are obtained at a deposition temperature of 700 °C. In parallel, promising barrier properties were demonstrated for such amorphous coatings, especially for the protection of titanium alloys from oxidation and corrosion at temperatures up to 600 °C.[4–6] These works revealed that, despite its instability and trend to ageing, ATI can be used for reproducibly depositing aluminum oxide provided that it is stored in a glove box, and renewed in the bubbler after a few hours of use. The next step towards industrial implementation of this process is the insight into the involved chemical reactions, and the determination of the corresponding reaction kinetics. Such knowledge allows process modeling, and hence controlling, and consequently optimizing, the relation between macroscopic processing conditions and the local deposition rates.

There are very few reports on local kinetic modeling of the MOCVD processes. This blank spot in processing science is due to the often complex chemical mechanisms involved, combining poorly known homogeneous and heterogeneous chemical reactions. The main difficulty then is to find representative chemical reactions and the related kinetic laws. Concerning the MOCVD of alumina from ATI, Kawase et al. experimentally investigated reaction kinetics in a hot-wall tubular reactor under 30 Torr total pressure in the temperature range 830–1160 °C.[7] Assuming a first-order reaction in ATI, they found an activation energy of 179 kJ mol^{-1}. They also obtained different deposition rates in two different tubular reactor diameters and concluded that the dominant reaction mechanism was the homogeneous pyrolysis of ATI. Hofman et al. performed CVD and mass spectroscopic experiments in this system operating under 3 Torr between 220 °C and 450 °C.[8] The authors showed that propene is a deposition by-product, and that the rate-limiting step is dehydration of the deposited AlOOH into Al_2O_3. They proposed a second-order reaction with an activation energy of 30 kJ mol^{-1}. Blittensdorf et al. used a stagnation point cold-wall CVD reactor to investigate the alumina deposition rate from ATI/O_2/Ar mixtures between 300 °C and 1080 °C, and under 35–190 Torr total pressure.[9] They found a temperature-independent deposition rate under 76 Torr and attributed this behavior to the decomposition of the precursor prior to reaching the substrate, i.e., deposition occurred in a gas-phase, starvation-limited process. In their experiments, Saraie et al. studied the influence of various atmospheres (N_2, N_2/O_2, N_2/H_2, N_2/H_2O) on the deposition rate of alumina from ATI in a hot-wall reactor, between 200 °C and 350 °C, under a total pressure 15 Torr, and proposed an activation energy of 80 kJ mol^{-1}.[10] More recently, Kawase and Miura performed experiments in two reactors with different diameters at 913 °C and at 1011 °C under a total pressure of 30 Torr and obtained different deposition rates, showing that the dominant reaction occurs in the gas phase.[11]

The discrepancy in literature results shows that the involved chemical mechanisms strongly depend on the adopted operating conditions, and especially on the deposition temperature and on the partial pressure of ATI. Most of the above-mentioned studies take for granted that the film composition is Al_2O_3 whatever the processing conditions, in contrast to the results reported by the authors' group.[1–3] Lee et al.,[12] operating in conditions close to the ones investigated in the present study, inferred that

[*] Prof. B. Caussat, Dr. H. Vergnes
Université de Toulouse, Laboratoire de Génie Chimique, ENSIACET/INPT 4, allée Emile Monso, BP 84234, 31030 Toulouse Cedex 4 (France)
E-mail: brigitte.caussat@ensiacet.fr
Dr C. Vahlas, D. Samélor, Prof. A. N. Gleizes
Université de Toulouse, Centre Interuniversitaire de Recherche et d'Ingénierie des Matériaux, ENSIACET/INPT
4, allée Emile Monso, BP 44362, 31030 Toulouse Cedex 4 (France)
E-mail: constantin.vahlas@ensiacet.fr

[**] This work was supported by the National Polytechnic Institute of Toulouse through a Bonus Qualité Recherche grant. We are indebted to Mr. Daniel Sadowski and to Miss Rosalia Vasquez Perez for technical assistance.

$Al(OH)_x$ species are deposited at 300 °C, and that the hydroxide species are removed by heating to 400 °C. Tentative kinetic analysis implicitly considered ATI as a monomer and postulated the formation of the hydroxides AlO(OH) (curiously written as O = Al–OH) or $Al(OH)_3$ as molecular species in the vapor phase,[13] however ATI has long been shown to be a tetramer ($[Al(O^iPr)]_4$) in the solid state, and to exist mainly as tetramer molecules in the vapor phase.[3] This is a key feature to consider when proposing relevant transitional species forming in the vapor phase.

This bibliographic survey reveals that the low pressure (LP)MOCVD process for the deposition of alumina from ATI in the temperature range 400–600 °C has only been fragmentarily investigated and, moreover, that the adopted basic assumptions are not validated. To the best of the authors' knowledge, local kinetic modeling of this CVD process has not yet been performed. This being the case, the aim of the present work is to develop a first local kinetic model of this process for the prediction of deposition rates in the operating range 450 °C–500 °C. This temperature range is technologically pertinent since it corresponds to moderate processing conditions leading to the formation of amorphous, stoichiometric alumina with excellent barrier properties. Four runs were performed using the same reactor temperature profile, nitrogen gas flow rate, and total pressure. Seven substrates were used per run, located between 8 cm and 36 cm from the reactor inlet. Bubbler temperature controlling the liquid ATI inlet mass fraction was the only varying parameter together with deposition time targeting comparable thickness of the films at similar positions from one run to the other. Assuming the gas stream to be saturated in ATI at the exit of the bubbler, the inlet flow rate of ATI in the deposition chamber, Q_{ATI}, was estimated from Equation 1 by Hersee and Ballingall.[14]

$$Q_{ATI} = Q_{N2,prec}\frac{P_{sat}(T_{sat})}{P_{reactor}-P_{sat}(T_{sat})} \quad (1)$$

$Q_{N2,prec}$ is the flow rate of nitrogen through the bubbler, $P_{sat}(T_{sat})$ the saturated vapor pressure at the evaporation temperature T_{sat}, and $P_{reactor}$ the operating total pressure. Equation 2 was used to determine the temperature-dependence of the saturated vapor pressure of ATI.[3]

$$\log_{10}(P_{sat}/\text{Torr}) = 11.35-4400/(T_{sat}/\text{K}) \quad (2)$$

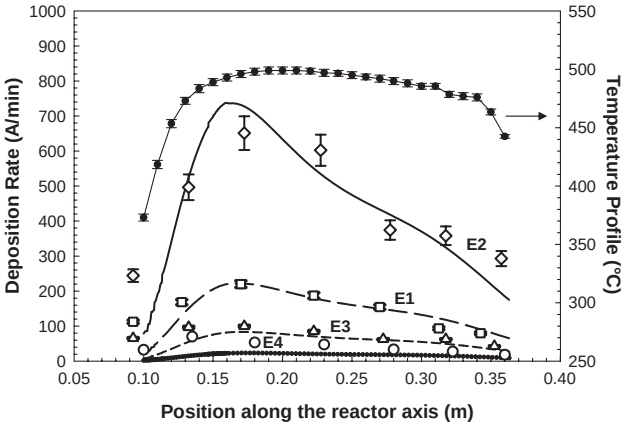

Fig. 1. Experimental axial evolution of the reactor temperature (full circles) and comparison between the experimental (E1: square, E2: diamond, E3: triangle, E4: circle) and calculated (E1: long dash, E2: solid line, E3: medium dash, E4: dotted) deposition rates along the reactor axis for runs E1, E2, E3, E4.

The corresponding Q_{ATI} values, together with the other processing conditions, are listed in Table 1. Films were 0.3 μm to 3 μm thick, depending on deposition time and on substrate location with respect to the precursor inlet.

Figure 1 presents the axial evolution of the temperature profile measured along the symmetry axis of the reactor, as well as the alumina deposition rates deduced from the mass difference in the substrates before and after deposition. The furnace and reactor features lead to a temperature profile containing a flat isothermal zone close to 490 °C between 0.15 and 0.25 m from the reactor inlet. Figure 1 shows that the axial evolution of the deposition rate is closely related to that of the reactor temperature for all bubbler temperatures studied.

Figure 1 also reveals a strong influence of the bubbler temperature, i.e., of the concentration of ATI in the deposition zone, on the alumina deposition rate. A ten degrees increase in the bubbler temperature results in a considerable increase in the deposition rate. For example, the maximum values of the latter at 90 °C and 110 °C are respectively 100 Å min^{-1} and 600 Å min^{-1}. An undesired consequence of the tested operating conditions is that the slope of the deposition rate evolution along the substrate length increases with increasing bubbler temperature. In other words, the higher the ATI bubbler temperature, the higher is the average deposition rate, but the deposition rate is less uniform along the substrate zone.

Table 1. Investigated operating conditions. Total pressure 5 Torr and total flow rate 653 sccm in all runs. Q_{ATI} calculated from Equations 1 and 2.

Experiment code	T_{sat} [°C]	Deposition time [min]	Q_{ATI} [sccm]	ATI molar fraction [10^{-2}]	ATI mass fraction [10^{-2}]
E_1	100	36	1.54	0.24	1.69
E_2	110	21	3.40	0.52	3.68
E_3	90	60	0.70	0.11	0.77
E_4	80	175	0.31	0.05	0.34

A mass balance, calculated between the provided atoms of Al in the input gas and the deposited Al atoms on the substrates and on the reactor walls, revealed that the ATI conversion did not exceed 50% under the tested conditions. This result will be discussed later in this article.

In order to develop a numerical model taking into account these results, the following apparent chemical heterogeneous reaction was considered; $[Al(OC_3H_7)_3]_{4(g)} \rightarrow 2\ Al_2O_{3(s)} + 12\ C_3H_{6(g)} + 6\ H_2O_{(g)}$. This reaction represents the entire homogeneous and heterogeneous chemical reactions involved. Hofman et al.[8] showed that the alumina deposition rate, R_{Di}, from ATI can be represented by the following apparent kinetic law, given in Equation 3.

$$R_{Di} = k_0 \exp(-E_a/RT)\,[ATI]^n \quad (3)$$

k_0 is a pre-exponential constant, E_a [J mol^{-1}] an activation energy, T [K] the temperature, and n the apparent reaction order (with R_{Di} in kg m^{-2} s^{-1}).

On the basis of this kinetic formulation, the results of experiments E_1, E_2, and E_3 were used to fit the three parameters k_0, E_a, and n. This fitting was performed by virtually dividing the LPCVD reactor into a series of perfectly mixed cylindrical reactors of 1 cm in length. The alumina deposition rate was assumed to be uniform in each compartment, i. An average value deduced from the weighing of each sample was considered for the substrate and for the reactor walls. Under these conditions, the following mass balance, given in Equation 4, was written for ATI.

$$Q_{i-1}\,y_{i-1} - Q_i\,y_i = \pm R_{Di}\,S_i \quad (4)$$

Q_i [kg s^{-1}] is the total gas mass flow rate, S_i is the deposition surface and y_i is the mass fraction of ATI in the i^{th} compartment. Q_i was calculated along the CVD reactor by considering the mass of alumina deposited. The inlet mass fraction of ATI at the first compartment was considered equal to the one provided by the bubbler at the reactor entrance. By minimizing the error between the experimentally determined deposition rate, R_{dexp}, and the calculated one, R_{Di}, for the three experiments, the following values of the kinetic parameters k_0, E_a, and n were obtained: $k_0 = 1.5 \times 10^6$ kg m$^{2.5}$ mol$^{-1.5}$ s^{-1}, $E_a = 78$ kJ mol^{-1}, $n = 1.5$.

This value of E_a corresponds to the main limiting phenomenon involved during ATI decomposition and alumina deposition for the conditions tested. As detailed above, Saraie et al.[10] obtained a very close value of 80 kJ mol^{-1} by operating between 220 °C and 450 °C under 15 Torr, with dry N_2 as the carrier gas. Hofman et al.[8] found 30 kJ mol^{-1} by operating between 230 °C and 440 °C under 3 Torr with dry N_2 as the carrier gas, however these works consider the composition of the films corresponding to pure Al_2O_3, whatever the temperature, without providing such evidence. The relevance of the literature values is thus questionable since it has been shown that, under similar processing conditions in the temperature range 350 °C – 415 °C, the film is hydroxylated, with a composition depending on deposition temperature. This temperature-dependence does not permit proposing any relevant activation energy from Arrhenius-type plots on too-large temperature domains. The apparent order of 1.5 proposed in this work reflects the dependence on ATI concentration of the dominant homogeneous and heterogeneous mechanisms existing in this range of operating conditions. It can be compared with the value 1 adopted by Kawase et al.[7] between 830 and 1160 °C and with the value 2 found by Hofman et al.[8] at temperatures slightly lower than the present ones. In the present state of the art, it is difficult to use more precise chemical and kinetic schemes.

With the aim of calculating local gas flow and species mass fractions in the presence of chemical reactions, the kinetic parameters k_0, E_a, and n were entered into the computational fluid dynamics (CFD) Fluent/Ansys® 12.1.4 code. Fluent is a pressure-based, implicit Reynolds number averaged Navier-Stokes solver that employs a cell-centered, finite-volume scheme, having second-order spatial accuracy. It discretizes any computational domain into elemental control volumes, and permits the use of quadrilateral or hexahedral, triangular or tetrahedral, and hybrid meshes. The following assumptions were made when using Fluent:

- Laminar gas flow (Reynolds number lower than 1000)
- Ideal gas
- No consideration of ATI in the evaluation of the physical properties of the inlet gas due to its low concentration
- No compressibility effects due to the low value (maximum 0.04) of the Mach number in the reactive zone
- No effect of the heats of reaction
- No activation of the energy equation. The temperature in the reactor was supposed to be uniform in the radial direction and its axial evolution was fixed equal to the experimental profile measured at the reactor center.

A 3D geometrical domain of 56,341 non-structured meshes was used to represent the whole reactive zone. The associated boundary conditions are the following:

- At the gas inlet, a flat profile was imposed on gas velocity
- At the symmetry axis and at the exit, classic Danckwerts conditions (diffusive flux densities equal to zero) were applied for gas velocity and mass fractions
- On the walls and substrate surfaces, a classical no-slip condition was used for gas velocity; the mass flux density of each species was assumed to be equal to the corresponding heterogeneous reaction rate
- At the exit, the total pressure was fixed at the experimental value

The physical properties of the gaseous mixture were calculated from the Fluent data base.

The experimental deposition rate profiles along the reactor axis for conditions corresponding to experiments E1, E2, and E3 are provided in Figure 2 together with the results obtained from modeling. The average relative error between the two sets of results for the three runs is close to 18%. This value can be attributed to the experimental errors of the deposition process, including uncertainty on the saturation pressure, and mainly to the adopted apparent kinetic law.

The elaborated model was used to simulate the deposition rate profile under the conditions of experiment E4 (not used for the establishment of the kinetic data). The obtained profile, together with the experimental deposition rates, are also reported in Figure 1. A satisfactory agreement is observed, which validates, as a first approach, the kinetic model for the investigated range of operating conditions.

Figure 2 presents local profiles of gas velocity (2a) and ATI mass fraction (2b) plotted along the vertical symmetry plane of the tubular reactor, and of the Al_2O_3 deposition rate along the substrate zone (2c). Operating conditions correspond to experiment E1, but the results are representative of all runs.

Gas flow presents a parabolic profile, characteristic of laminar flow both in the entrance tube and in the deposition zone. The gas mean velocity is close to $70\,m\,s^{-1}$ in the entrance tube, and to $20\,m\,s^{-1}$ in the deposition zone. These values correspond to a very short residence time of several tens of milliseconds for the gas in the reactive zone. Under these conditions, the convective contribution clearly dominates the diffusive one for gas flow, and also for thermal and mass transfers.

Due to the low concentration of ATI in the input gas, more than 98% of the gas is composed of nitrogen. The conversion of ATI was calculated to be 39%, 50%, and 30% for runs E1, E2, and E3, respectively. It is concluded that the conversion of ATI decreases with increasing the inlet ATI mass fraction. These relatively low values of ATI conversion are attributed to the low deposition temperature and to the very short residence time of gaseous species in the reactive zone. Local mass fraction profiles for all species show parabolic evolutions due to the dominance of the convective part. Depletion in ATI mass fraction of roughly 35% is observed for run E1 between the beginning and the end of the reactor zone containing the substrates. Such depletion is responsible for significant axial variations of the deposition rate, as illustrated in Figure 2c. Uniform low values of deposition rates were obtained from 40 cm after the reactor inlet (as was also observed experimentally) because the temperature is lower than 250 °C.

Figure 3 presents a surface optical micrograph of the deposition after run E1. The observed iridescence reveals the inhomogeneous thickness of the film. Deposition rate profiles from simulation reproduce this iridescence qualitatively, as can be seen in Figure 2c. This inhomogeneity is certainly due to the depletion of ATI in conditions of high gaseous convective fluxes.

In conclusion, a local kinetic model for the MOCVD of alumina from ATI, based on an apparent heterogeneous

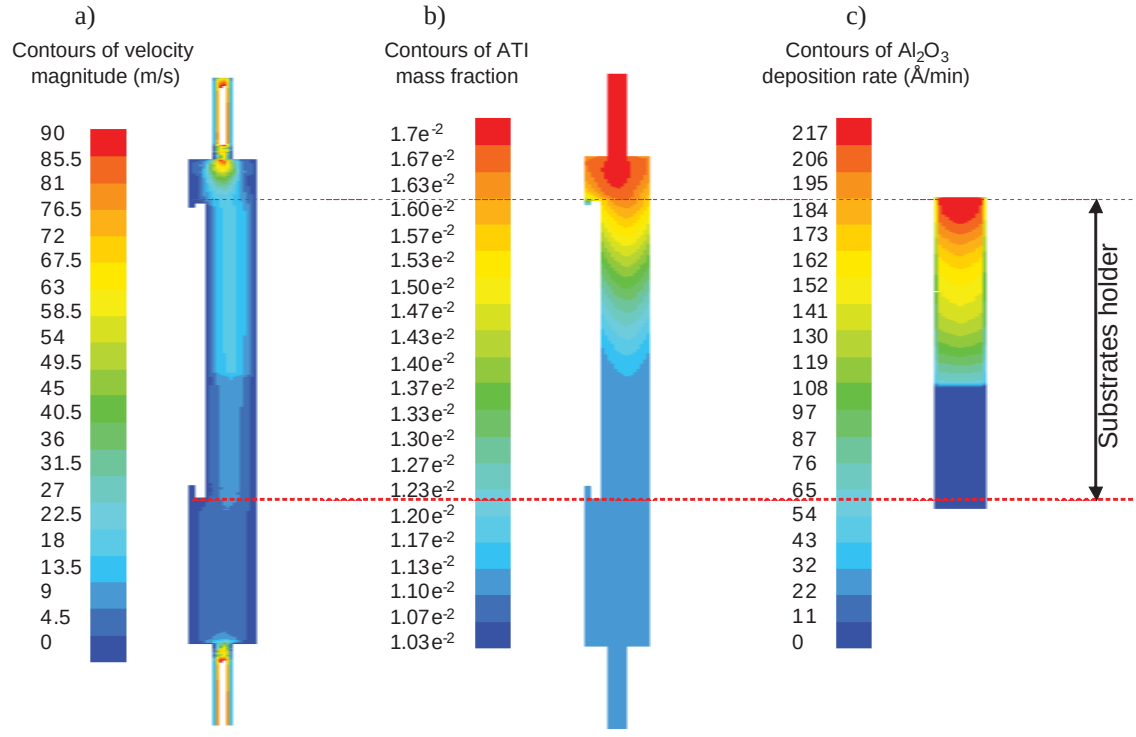

Fig. 2. Calculated local evolutions of a) gas flow, b) ATI mass fraction along the vertical symmetry plane of the reactor, and c) alumina deposition rate along the substrate zone.

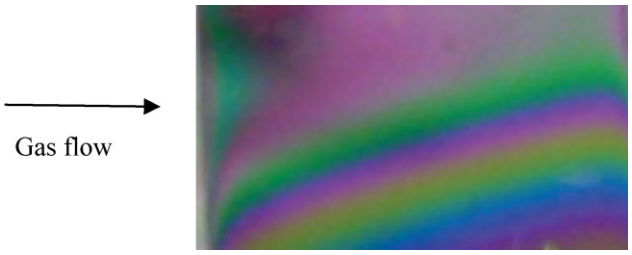

Fig. 3. Photograph of a 15 mm × 10 mm substrate after alumina deposition for run E1 at position 0.31 m along the reactor.

kinetic law from Hofman et al.,[8] was developed using the CFD code Fluent. The kinetic parameters were fitted from experimental deposition rates obtained between 360 °C and 496 °C, under a total pressure of 5 Torr, for three different ATI bubbler temperatures, corresponding to three concentrations of the precursor in the input gas. The model was validated by comparison with experimental results from an additional experiment performed under the same range of operating parameters. Local profiles of gas flow, species mass fractions, and alumina deposition rates were analyzed, permitting the reproduction of the non-uniformity of deposition rate due to the convective gas transport and depletion of ATI.

Despite the use of an apparent heterogeneous chemical reaction, the adopted 3D model presents potential for the optimization of process behavior in the operating range of interest, in particular in the prospect of treating complex-shaped pieces. The proposed approach is subjected to improvement through additional experimental information and can be generalized to other MOCVD processes.

Experimental

Experiments were performed under 5 Torr, in a horizontal, hot-wall, tubular CVD reactor heated by a Trans Temp transparent furnace, as detailed elsewhere [1]. Such a furnace ensures an efficient thermal transfer between reactor walls and substrates by radiation, and minimizes the temperature difference between them. As-received ATI (Acros Organics) was melted in its bubbler at 140 °C and was kept as a supercooled liquid at 60 °C between each experiment. It was operated between 80 °C and 110 °C, depending on the requested vapor pressure, and was carried to the deposition zone by 99.9992% pure N_2 carrier gas (Air Products).

The films were deposited on 15 mm × 10 mm, or on 8 mm × 10 mm, silicon substrates. Substrates were weighed before and after the alumina deposition using a Sartorius balance (± 10 μg) to determine the deposition rate of the films. A sample holder was machined in a AU4G (AlCu4MgSs) aluminum alloy plate with dimensions 1 mm × 358 mm × 19 mm. Before deposition, the samples were degreased in acetone for 5 min, rinsed with ethanol for 5 min, and with deionized water, and finally dried in Ar flow. Each substrate was placed on the sample holder at predefined positions.

Received: December 17, 2010
Revised: April 27, 2011

[1] A. Gleizes, C. Vahlas, M. M. Sovar, D. Samélor, M. C. Lafont, *Chem. Vap. Deposition* **2007**, *13*, 23.
[2] A. M. Huntz, M. Andrieux, C. Vahlas, M. M. Sovar, D. Samélor, A. N. Gleizes, *J. Electrochem. Soc.* **2007**, *154*, P63.
[3] M. M. Sovar, D. Samélor, A. N. Gleizes, C. Vahlas, *Surf. Coat. Technol.* **2007**, *201*, 9159.
[4] J. D. Béguin, D. Samélor, C. Vahlas, A. N. Gleizes, J. A. Petit, B. Sheldon, *Mater. Sci. Forum* **2008**, *595*, 719.
[5] G. Boisier, M. Raciulete, D. Samélor, N. Pébère, A. N. Gleizes, C. Vahlas, *Electrochem. Solid State Lett.* **2008**, *11*, C55.
[6] D. Samélor, M. Aufray, L. Lacroix, Y. Balcaen, J. Alexis, H. Vergnes, D. Poquillon, J. D. Beguin, N. Pébère, S. Marcelin, B. Caussat, C. Vahlas, *Adv. Sci. Technol.* **2010**, *66*, 66.
[7] M. Kawase, Y. Ikuta, T. Tago, T. Masuda, K. Hashimoto, *Schem. Eng. Sci.* **1994**, *49*, 4861.
[8] R. Hofman, R. W. J. Morssinkhof, T. Fransen, J. G. F. Westheim, P. J. Gellings, *Mater. Manuf. Processes* **1993**, *8*, 315.
[9] S. Blittersdorf, N. Bahlawane, K. Kohse-Höinghaus, B. Atakan, J. Müller, *Chem. Vap. Deposition* **2003**, *9*, 194.
[10] J. Saraie, K. Ono, S. Takeuchi, *J. Electrochem. Soc.* **1989**, *136*, 3139.
[11] M. Kawase, K. Miura, *Thin Solid Films* **2006**, *498*, 25.
[12] D. H. Lee, D. J. Choi, S. H. Hyun, *J. Mater. Sci. Lett.* **1996**, *15*, 96.
[13] G. P. Shulman, M. Trusty, J. H. Vickers, *J. Org. Chem.* **1963**, *28*, 907.
[14] S. D. Hersee, J. M. Ballingall, *J. Vac. Sci. Technol.* **1989**, *A8*, 800.